Geomechanics and Engineering, *Vol. 23, No. 4 (2020) 381-392*
DOI: https://doi.org/10.12989/gae.2020.23.4.381

Contribution of modification of a pressuremeter for an effective prediction of soil deformability

Soufyane Aissaoui[1a], Abdeldjalil Zadjaoui[*1] and Philippe Reiffsteck[2b]

[1]*Department of Civil Engineering, Tlemcen University, 22 rue Abi Ayed Abdelkrim, Fg Pasteur BP 119. 13000, Algeria*
[2]*IFSTTAR-Paris, 14-20 Boulevard Newton Cité Descartes, Champs sur Marne F-77447, Marne la Vallée Cedex 2, France*

(Received July 4, 2019, Revised November 4, 2020, Accepted November 7, 2020)

Abstract. The difficulties, challenges and limitations faced in standard pressuremeter testing in the measurement of low soil deformations led a number of researchers to think about the possible modification of the equipment, and especially the replacement of the volumeter by a Hall Effect sensor. This article is a major contribution in this direction. It makes an attempt to detail the design, manufacture and operation of the new equipment. The calibration of the various components was carried out according to the rules presently in force. This proposal was applied, on an exploratory basis, to the data of a real site located in France. The authors present the preliminary results of some cyclic pressuremeter tests, previously carried out in the laboratory, on a sandy material, and they then provide a basic interpretation of these results. The findings indicated that the proposed apparatus is capable of providing high-quality information about constraints and deformations. Although these tests were performed within the laboratory, it was possible to analyze the power, quality, performance and insufficiencies of the proposed equipment.

Keywords: soils; in-situ equipment; pressuremeter; testing of materials; measuring feeler; cyclic stress-strain

1. Introduction

Soil mechanical parameters can be determined in the laboratory, on specimens taken from the field, or directly in situ, by means of pressuremeter or penetration tests (Tarawneh *et al.* 2018). Currently, field trials are preferred by practitioners and are routinely performed during a geotechnical study (Clarke 1995, Aziz and Akbar 2017) because, unlike those performed in the laboratory, they offer the advantage of not requiring sampling and therefore not distorting the results obtained due to a poorly performed sampling. Nevertheless, these tests have a serious disadvantage since the practitioner cannot fully control the environment during the test, and therefore he may lose certain information that the laboratory tests could easily provide.

Recent developments in the field of civil engineering have generated multiple problems of interaction between structures and soils, especially during the construction of large structures in cities and in their subsoil as well (Borel and Reiffsteck 2006). The interactions between soils and structures give essentially problems of compatibility of deformations that can only be reliably treated when the deformability of different soils at low levels of deformation are known. In order to directly control the deformations of soils and structures, and their interactions, a great deal of research has been conducted on the development of new devices for in-situ soil control; among these, it is worth mentioning the penetrometers, dilatometers and pressuremeters, which have been reported in the works of Zhou (1997), Akbar (2001), Reiffsteck and Borel (2002), Arbaoui (2003), Reiffsteck *et al.* (2005), Thorel *et al.* (2007), Rehman (2010), Barry *et al.* (2012), Johnston *et al.* (2013), Shaban and Cosentino (2017), Wang *et al.* (2018), Masoud and Khan (2019), etc. These devices were developed to determine better soil parameters. In addition, an approach was devised for the purpose of deriving, from the test, certain data that can be effectively used in geotechnical monitoring and engineering calculations.

For the purpose of improving the methods of measuring soil deformability, it seemed advisable to go further in the in-situ testing, especially because the in-situ tests currently occupy a prominent place in today's geotechnical studies. Among these tests, it would be interesting to mention the pressuremeter test, which is considered as the most widely used in-situ soil investigation tool for calculating and optimizing foundations (Baguelin *et al.* 1978, Amar *et al.* 1991, Gambin 1990, Likitlersuang *et al.* 2013). Note that Kögler (1933) was the first person to perform the cylindrical probe expansion test to measure soil characteristics. This essay reached its current growth only under the impulse of Louis-François-Auguste on January 19, 1955 at 15h 6 mn, the moment when this person deposited a patent for invention with the number 1.117.983 (Ménard, 1955). According to this invention, the principle of in-situ experimentation consists of introducing a diametrically deformable cylindrical cell into a borehole at

∗Corresponding author, Professor
E-mail: a.zadjaoui@gmail.com
[a]Ph.D. Student
E-mail: aissaouisoufyane@yahoo.fr
[b]Professor
E-mail: philippe.reiffsteck@ifsttar.fr

ISSN: 2005-307X (Print), 2092-6219 (Online)

Table 1 Geometric characteristics of the probe

			Notation	Value	Tolerance
Flexible sheath probe	Central cell	Length (mm)	l_s	210	[0; +5]
		Outside diameter (mm)	d_s	58	[-2; +2]
	Guard cell	Length (mm)	l_g	120	[-15; +15]
		Outside diameter (mm)	d_g	58	[-2; +2]

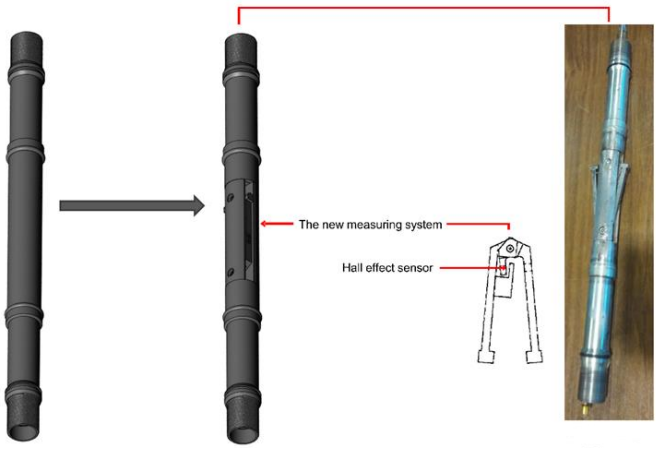

Fig. 1 Principle of the developed design model

staggered depth values. The diameter of this cell must correspond to that of the borehole, but without proper elastic reaction. The cell is inflated, with an incompressible fluid, on demand and according to a well-defined "pressure-time" program (Oztoprak *et al.* 2018).

Several works have contributed to the development of this test and to the popularization of its use, Jézéquel and Touzé (1970) filed a patent entitled "Pressiometric drilling probe". Indeed, these two authors tried to eliminate the reworking operations that are due to the Menard Pressuremeter test during predrilling with self-boring (Baguelin and Jézéquel 1973). This idea also emerged at the same time in Cambridge in the United Kingdom, and later culminating in the Camkometer, which is a self-boring pressuremeter, with some specificities related to its slenderness, and to its ability to measure deformations (Wroth and Hughes 1972, Windle and Wroth 1977). Other types of cone pressuremeters were later developed. Moreover, Briaud and Shields (1979) from the University of Ottawa (Canada) made the first attempt to develop a single-cell probe that can be set up by threshing or jacking in the ground for the characterization of streets, roads and airfields (the pavement pressuremeter). The most popular model of this type of pressuremeter is the PENCEL Pressuremeter, manufactured by the Canadian company Roctest (Messaoud and Cosentino 2016). With the growing interest in offshore design and the consequent need for accurate measurements of in-situ properties of offshore clays, Reid *et al.* (1982) developed a push-in pressuremeter. Thereafter, Withers *et al.* (1986) in England developed the full-displacement pressuremeter which was later further developed and tested in Canada by Campanella and Robertson (1986), Italy Ghionna *et al.* (1995) and in Holland by Zuidberg and Post (1995).

These latest developments exhibit several flaws; they are expensive and cannot be used in all types of soils. For this, an alternative way of improvement would be to work on the deformation measurement at the wall of the probe; this method is more accurate than working on a burette, even if it is instrumented. A detailed discussion on the development of a new generation of pressuremeters to provide richer information on small deformations are provided in this article. The methodology, calibration and validation of the first results are also presented in detail.

2. Development and design

2.1 Description of the Menard pressuremeter

The main body of the probe is made of high-strength stainless steel. The core of the probe consists of a single metal cylinder serving as support for three cells: two guard cells of length equal to 120 mm each, and a central measuring cell of length 210 mm; the three cells are coated with a rubber sheath. The probe has an inside diameter of 31 mm, and an outside diameter of 58 mm (with the membrane); both ends of the main body are identical. One end is connected to the pressure-volume controller via semi-rigid tubing, to ensure the passage of gas to the central measuring cell. However, the other end is protected by a sabot.

2.2 Developed design model

The basic design principle of the new equipment developed is schematically illustrated in Fig. 1 Indeed, a standard Ménard probe of diameter equal to 58 mm is used.

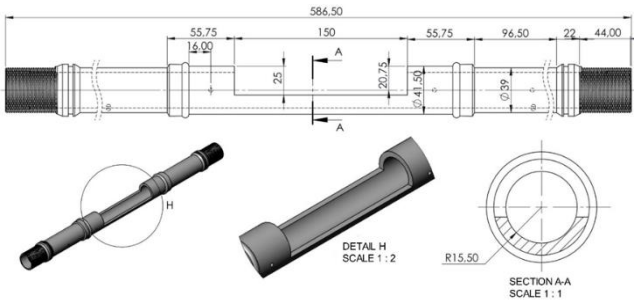

Fig. 2 Description of the measurement area (dimensions in mm)

Fig. 3 Creation of the measurement zone

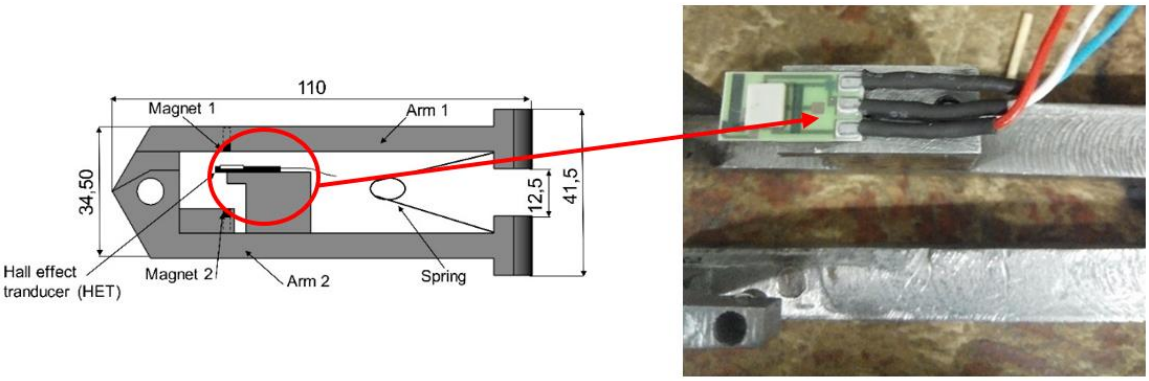

(a) (b)

Fig. 4 (a) Measuring range of the feeler and (b) Position of the Hall Effect sensor

It consists of three cylindrical cells with a circular cross-section and mounted on the same axis; the geometric characteristics of the probe are given in Table 1.

A test plate was implanted inside the central measuring cell. Then a new measurement system (measuring feeler) was incorporated into the body of the standard probe. This measuring feeler is equipped with a Hall Effect sensor; its role is to control and monitor the expansion of the membrane when performing a pressuremeter test. The area to be opened in the central measurement cell is clearly shown in Fig. 2 This part of the cell is sealed, which makes it possible to prevent any leakage from the gas-bearing circuit. Moreover, the opening created in the cell is 150 mm long and is positioned in the middle of the probe to allow the user to take measurements at the midpoint of the membrane.

The diameter of the central cell is equal to 41.5 mm, and the opening was made with a depth h equal to 25 mm, as is clearly illustrated in Fig. 2 Note that the tube that connects the two guards cells and which is used to transfer gas from the first guard cell to the second guard cell must not be touched. A new measurement system was subsequently placed between these two guard cells.

2.3 Manufacture of the first prototype

A structural steel alloy with low contents of nickel, chromium, molybdenum (36NiCrMo16) was used for the

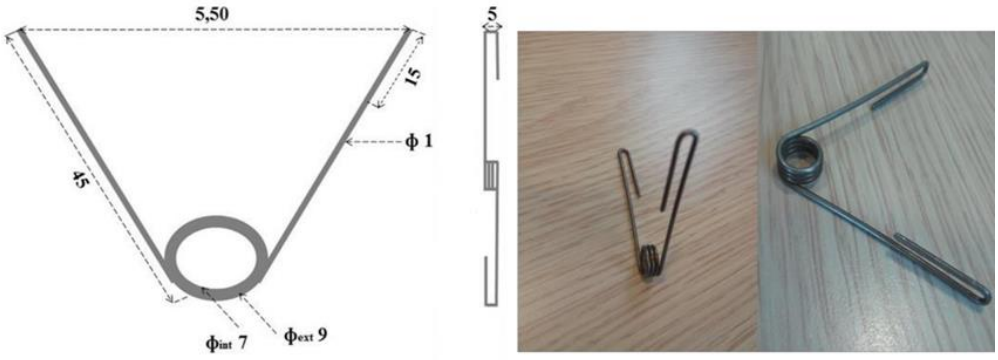

Fig. 5 Detailed diagram of the spring

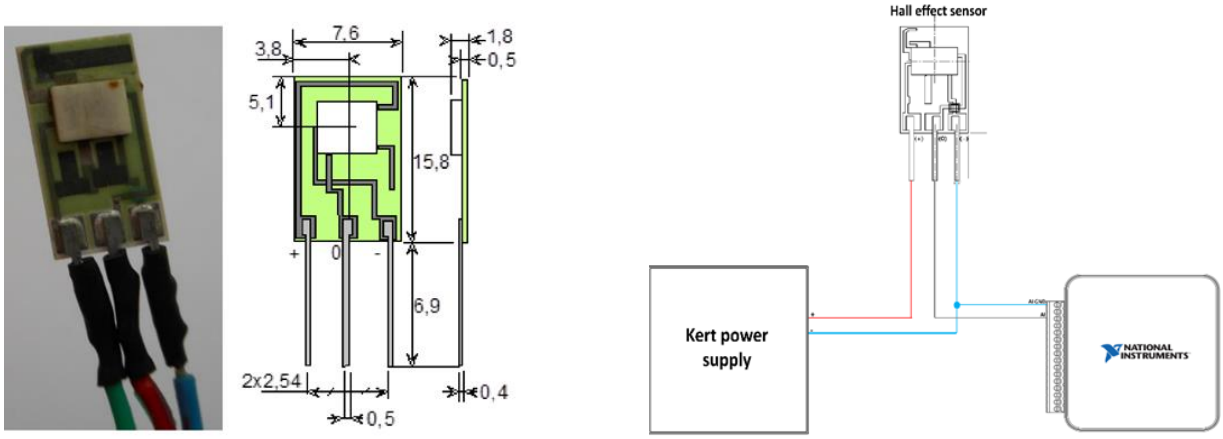

(a) (b)

Fig. 6 (a) Ratiometric Hall Effect sensor and (b) Setup of the Hall effect sensor

manufacture of the different parts of the prototype in order to achieve very high mechanical characteristics while offering maximum safety.

The production of the first prototype of the model developed was completed in the mechanical manufacturing workshop of Mr. OTMANI Mohammed, located in Ain Defla in the city of Tlemcen (Algeria). The first task consisted of creating the measurement zone in the center cell, as shown in Fig. 3.

2.4 Deformation measurement system

The device used to measure and control the displacement of the membrane is a measuring feeler which is made of high strength stainless steel (36NiCrMo16). It consists of two arms and a seat for the Hall Effect sensor. In the initial position (no membrane expansion), the distance between the outer ends of the two arms (upper and lower) of the measuring feeler is equal to that of the inner diameter of that probe (i.e., 41.5 mm), as depicted in Fig. 4(a). The arms can stretch out radially within a range extending between 41.5 mm and 71.5 mm.

The Hall Effect sensor is positioned on a support placed appropriately between the two magnets of arm 1 (Fig. 4(b)). The dimensions of the sensor support allow the user to cover a measurement range of about 30 mm. This value corresponds to the maximum limit that the device can reach, which means when the portion carrying magnet 2 comes into contact with the Hall effet sensor support.

A helical torsion spring was used between the two arms of the feeler. This spring has the essential role of restoring a torque; work is done when the spring rotates (Fig. 5). The fixing system of this type of spring is simple, which allows it to have a very wide range of applications.

3. Calibration of the measuring system

Calibration was performed for the electronic part of the equipment used. This makes it possible to convert the analog output units to pressure and radial expansion units during a pressuremeter test and also to ensure proper functioning of the equipment.

3.1 Calibration of the displacement sensor

The probe membrane displacement measurements were achieved with the newest technologies which are based on Hall Effect sensors. The main advantage of using this type of sensors lies in the fact that it allows measuring a position or a lateral displacement through a non-ferromagnetic wall separating the probe from the magnet support.

The principle of operation of the sensor is based on the fact that when a semiconductor is crossed by a current, it is

Fig. 7 Diagram for the calibration setup

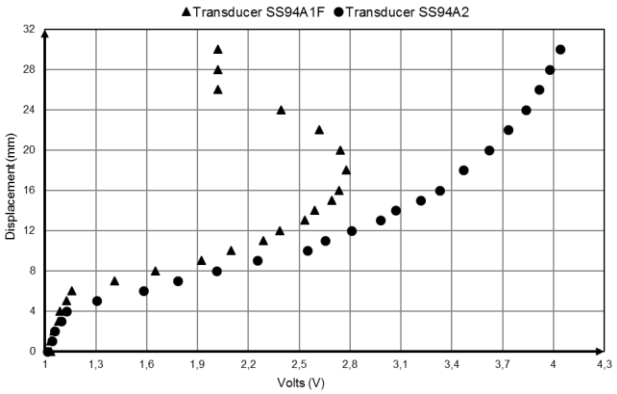

Fig. 8 Comparison of the results obtained by SS94A1F and SS94A2 sensors

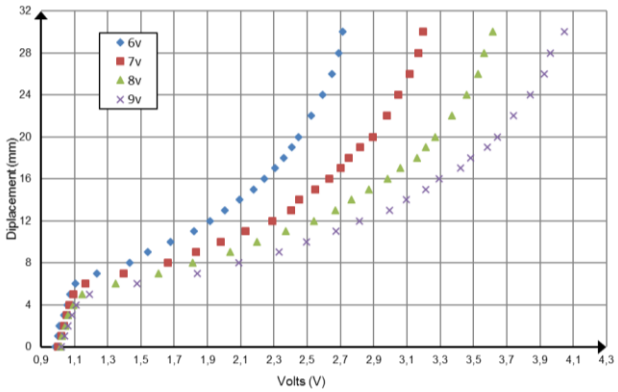

Fig. 9 Hall Effect sensor calibration curve, for different voltages

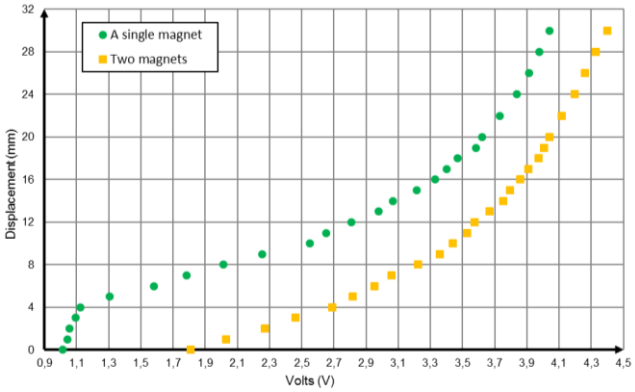

Fig. 10 Influence of the magnetic polarization on the sensor response

subjected to a magnetic field whose lines of force are perpendicular to both the plate and the current; also, any displacement in the direction of current would generate a DC voltage that is proportional to the magnetic field.

3.1.1 Setup

The sensor used in this study is a Honeywell Ratiometric linear Hall Effect sensor (Fig. 6(a)), made of ceramic, which produces an output voltage proportional to the intensity of the magnetic field to which it is exposed; it is compensated in sensitivity and temperature. The sensor is supplied with DC voltage using a 0-15V KERT power supply that is connected between the positive terminal (+) and the negative terminal (-) which is connected to ground. The third one (0) is used when the ground is taken as a reference, with zero potential (Fig. 6(b)).

3.1.2 Methodology

The calibration of the radial movement of the feeler-arms, to prevent any change in the sensor output, was done prior to the placement of the probe membrane. After that, the relationship between the voltage emitted by the sensor, and recorded by the National Instruments acquisition box, and the radial movement of the feeler-arms must be established.

The probe, with all its components, was fixed in a horizontal position in order to perform the calibration. Then, a digital caliper was used to measure the relative movement of the arm (Fig. 7). Note that the measurements were realized and recorded every millimeter, until the maximum range of arm movement (30 mm) was reached. The operation was performed on one feeler-arm, while the other one remained fixed.

At first, the calibration operation was carried out using two sensors with different references, i.e., SS94A1F and SS94A2, in order to see the influence of the sensor type on the results found. The difference resulting from the use of the two sensors lies in the interval of measurement of the magnetic field intensity. Indeed, the sensor SS94A1F allows for the measurement of the magnetic field within the interval [-100, +100] Gauss, while the sensor SS94A2 does it within the interval [-500, +500] Gauss. The results given by the first test are summarized in Fig. 8.

As is clearly indicated in Fig. 8, the sensor SS94A1F can no longer detect any magnetic field, which means that the movements of the measuring feeler cannot be detected and measured beyond the position of 18 mm. On the other hand, the sensor SS94A2 gives voltage variations up to the position of 30 mm. This is the reason why it was decided to use the SS94A2 sensor in order to have the maximum measuring range.

In order to be able to assess the influence of the supply voltage change on the measurement range, it was deemed interesting to carry out a parametric study. For this, the different phases involved in the sensor calibration process were repeated for different voltage values, i.e., 6V, 7V, 8V, and 9V. The results obtained are summarized in Fig. 9. This

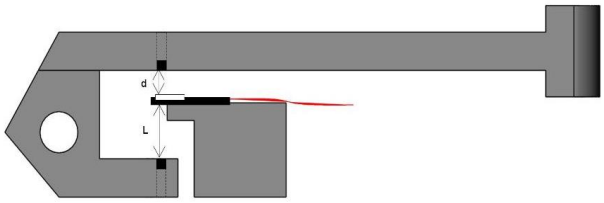

Fig. 11 Representation of the position of the magnet relative to the Hall Effect sensor

b e

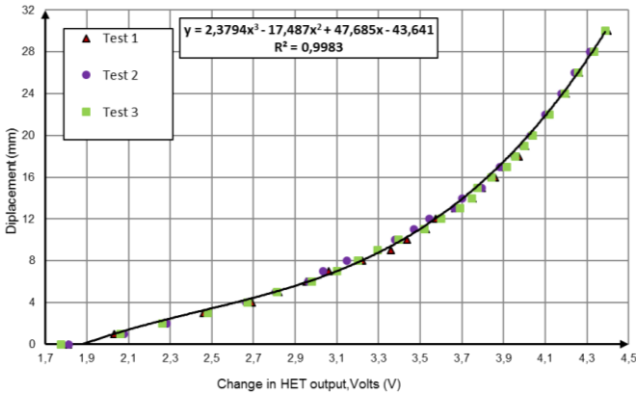

Fig. 12 Relationship between the output voltage and the measuring feeler movement

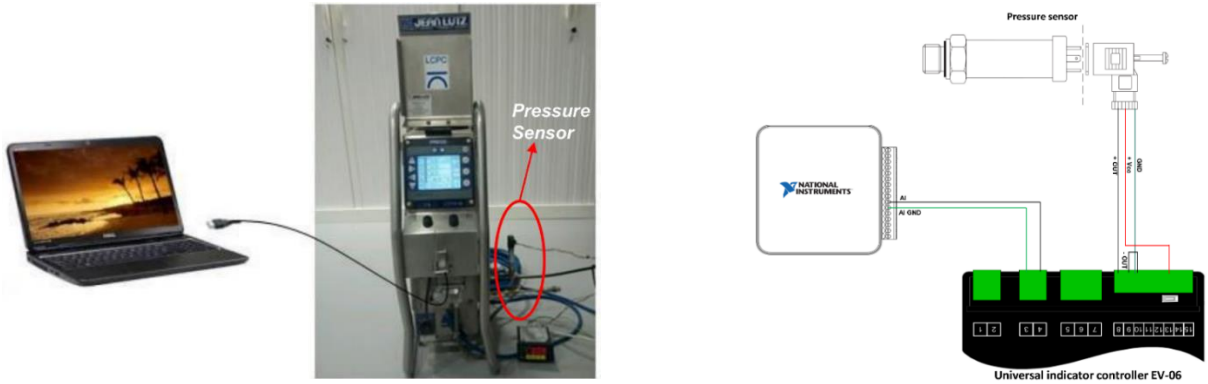

(a) (b)

Fig. 13 (a) Connection of the pressure sensor and (b) The pressure sensor setup

figure shows that for each voltage increase, the measuring range of the sensor rises. For example, for the voltage of 6V, the measuring range is 1.728 V; but for the voltage of 9V, the measuring range is 3.025 V. For this reason, it was decided to opt for the use of the 9 V supply voltage.

It was found that the variation of the Hall Effect sensor response as a function of the magnetic polarization was significant. For this reason, it was decided to carry out a calibration operation with two types of polarizations. The first type consisted of using only the magnet of the upper part, but in the second one, the two magnets were used in order to determine the influence on the sensor response, as illustrated in Fig.10. It is worth noting the good linearity of the signal in the case where two magnets with different poles are used (north-south or south-north). It should also be mentioned that in the second case, for the interval from 0 to 4 mm, the response of the sensor is faster, and has a better sensitivity as compared to the first case. Therefore, the second type of polarization is much more interesting to used for the calculation of small deformations. This is the reason why it was decided to opt for the second configuration.

Furthermore, a parametric study was performed on the second configuration, but with different positions of the magnet with respect to the Hall Effect sensor; this was done until a sufficiently linear response of the sensor was attained (Fig. 11).

The power source was kept fixed at 9 V during the calibration test. The position of the upper magnet (d) was changed with respect to the Hall Effect sensor. It was observed that each time the position of the magnet was changed, bringing it gradually closer to the magnet of the sensor, the non-linearity of the sensor response decreased and the degree of the polynomial trending went down, while the coefficient R2 moved closer to unity.

In addition, the configuration (d = 4 mm, L = 9.5 mm), which gave us a better linearity with R2 = 0.999, was considered. Then, the calibration was repeated for this last

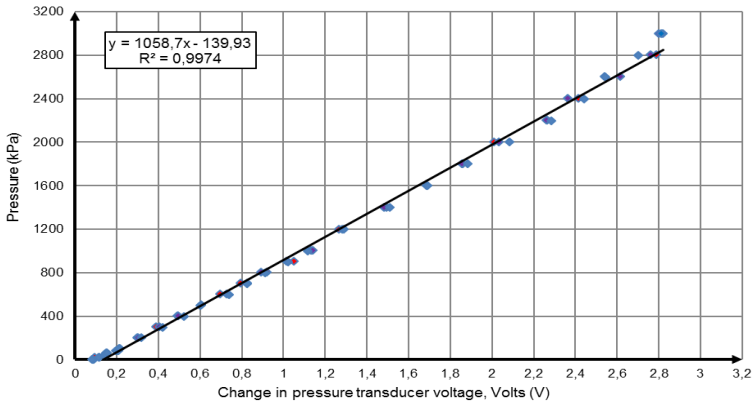

Fig. 14 Calibration curve of the pressure sensor

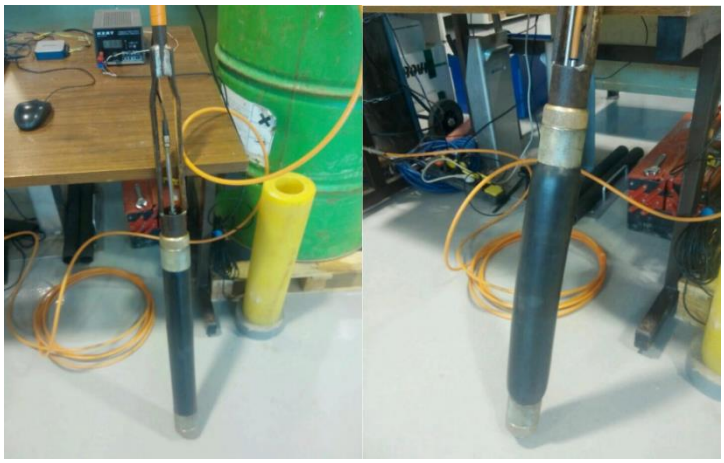

Fig. 15 Pressuremeter probe during the calibration phase

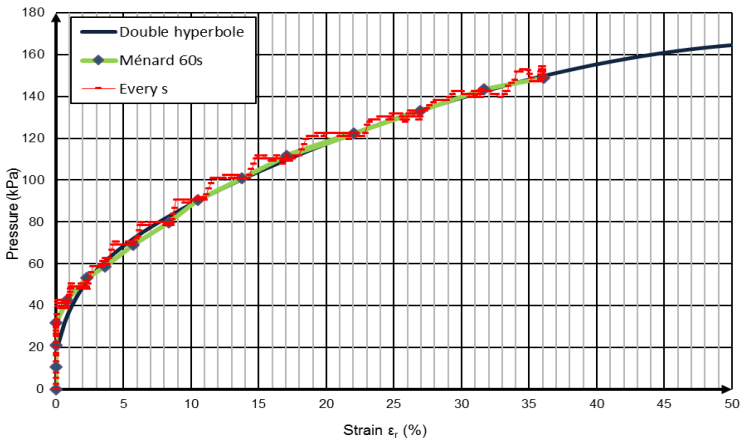

Fig. 16 The membrane calibration curve

configuration three times successively, as is clearly shown in Fig. 12 below, and the results found seemed consistent.

3.2 Calibration of the pressure sensor

The objective was to achieve a good accuracy essentially in the measurements of the pressure applied to the probe. For this, a KELLER electric sensor was used instead of the commonly used blade manometers. Its main function is to determine the pressure and transmit it to a recorder.

This type of pressure sensors provides the user with precision, stability and reliability. It is used in typical applications such as refrigeration temperature controllers, air compressors, hydraulic circuits, and vacuum pumps. The pressure sensitive element in the sensor is a piezo-resistive micro-machined silicon chip, of high stability, mounted floating on the filling oil of the sensor which is closed by a thin separation membrane which receives the pressure to be measured.

3.2.1 Sensor setup with the EV-06 recorder

The pressure sensor was positioned on the pressure-volume controller (Fig. 13(a)). Note that it can be placed anywhere on the air pressurization circuit. A three-wire power cable was used to connect the end of the pressure sensor to the EV-06 recorder, and then the recorder to the data acquisition box (Fig. 13(b)).

3.2.2 Calibration methodology

The calibration procedure for the pressure sensor is the same as that used for the Hall Effect sensor. Constant pressure values were applied for 30 seconds and the voltage corresponding to each value of the pressure was measured with the EV-06 recorder and the data acquisition software. In addition, the preliminary calibration of the pressure sensor was carried out using a Jean Lutz controller. The amplitude of the pressure stages was chosen at a maximum of 3 MPa; the monitoring operation was carried out from a log file with the help of a specific control software (PREVO) installed on a laptop that is connected to the controller through a USB cable.

The results of the calibration operation are summarized in Fig. 14, with the equation of the line obtained by linear regression and which must be introduced into the SignalExpress software. There is a rapid and substantially linear variation of the voltage as a function of the applied pressure. The test was repeated three times, and the results obtained seemed consistent. As can be seen on the calibration curve, the abscissa at the origin, that is to say the value at zero pressure, is equal to 0.08V; it corresponds to the atmospheric pressure.

3.3 Membrane stiffness correction

A correction of the membrane stiffness was made (Fig. 15) to take into account only the actual pressure affecting the soil sample during the pressuremeter test.

Fig. 16 shows the curve of the membrane stiffness calibration at t = 1 s and t = 60 s. The same figure shows the double-hyperbolic curve which schematizes the appearance of the shape of the calibration curve. The value of the corrected pressure can be deduced directly from the raw pressure which itself may be derived from the calibration pressure using the following expression:

$$p_c = p_r - p_e \quad (1)$$

where p_c is the corrected pressure, pr is the pressure at controller and pe the pressure due to the membrane stiffness.

The correction is given by the expression of the following double hyperbolic curve:

$$p = A_1 + A_2 * \varepsilon_r + \frac{A_3}{A_5 - \varepsilon_r +} + \frac{A_4}{A_6 - \varepsilon_r} \quad (2)$$

The iteration process was performed using Microsoft Excel, to obtain the 6 parameters A_i, with i = 1 to 6, which relate the pressure (p) to the deformation (ε_r).

A_1 = 2,495; A_2 = 0,052; A_3 = 0,002; A_4 = -227,416; A_5 = -0,010; A_6 = 99,826

4. Testing

The initial experimental approach consisted in conducting the validation tests in order to check for the limits of the developed equipment. For purely experimental reasons (simplicity, control, homogeneity, etc.), it was decided to opt for the use of a sandy material, with known behavior and characteristics, placed in a metal tank in such a way that the prototype simulates the actual testing conditions. The tank used was filled with sandy soil from the Seine River, brought from the SRO laboratory of IFSTTAR in France. The characteristics of this type of sand are summarized in Table 2.

4.1 Measurement protocol and sample preparation

The principle of the test was to measure the deformation of soil while applying the various pressure cycles. The idea consisted of estimating the radial deformation of soil as a function of the pressure cycles, by using a measuring feeler

Table 2 Characteristics of the sand used

D_{50} (mm)	C_u	e_{min}	e_{max}	ρ_s (g/cm^3)	ρ_{dmin} (g/cm^3)	ρ_{max} (g/cm^3)
0,71	6,33	0,423	0,568	2,65	1,690	1,861

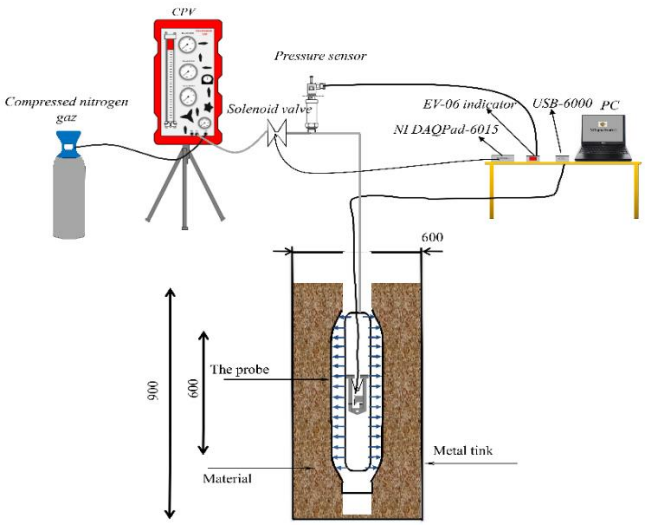

Fig. 17 Architectures envisaged and test principle with the developed probe

Fig. 18 Overview of the PANDA 3® Labo Penetrometer

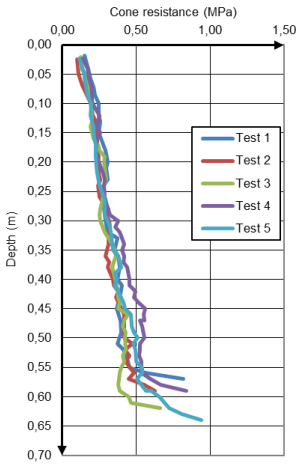

Fig. 19 Variation of dynamic resistance as a function of depth

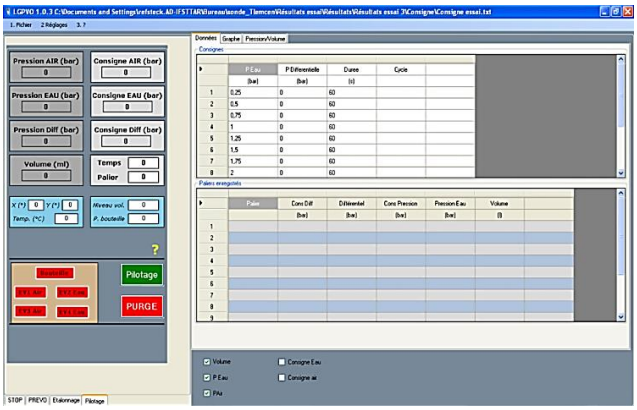

Fig. 20 Screenshot of the control program

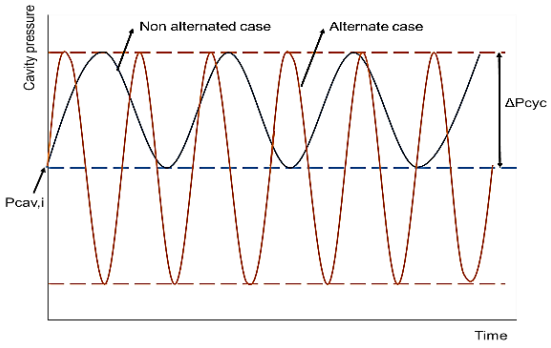

Fig. 21 Parameters of cyclic loading

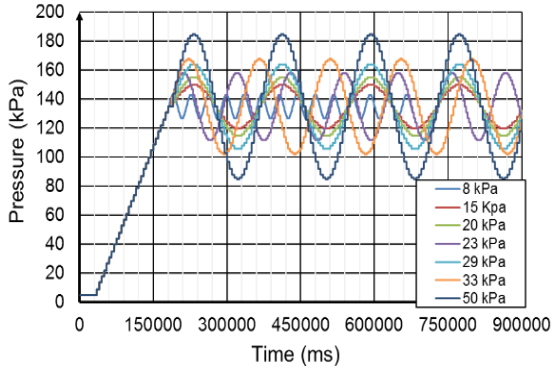

Fig. 22 Cyclic loading setpoint for multiple values of ΔPcyc

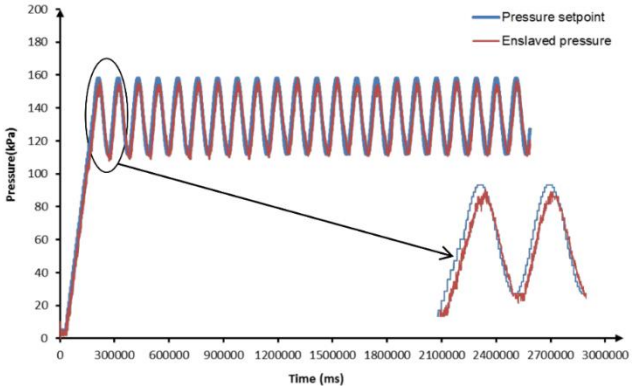

Fig. 23 Comparison of the setpoint signal and pressure measurement

equipped with a Hall Effect sensor, instead of deducing the displacements from the variations of a fluid volume (Fig. 17).

Penetrometer tests with PANDA 3® Labo (Dynamic Digital Autonomous penetrometer) were carried out before each test with the modified pressuremeter probe, as shown in Fig. 18. The objective was to formulate soil test pieces that guarantee the homogeneity of the relative density (the test pieces have constant relative density). The relative density is an important quantity for the rigorous control of relevance, feasibility and repeatability of the developed probe.

4.2 Results and discussions

The correlation between the relative density and resistance to dynamic penetration was used in order to find the sand density. It is obvious that if the results of the different tests give the same dynamic resistance, it means that this should also be true for the density. Fig. 19 illustrates the curves obtained for the various tests carried out in the sand tank.

The penetrograms obtained show, at first sight, that the soil used in the laboratory is of relatively good quality, which indicates that it has a good homogeneity since the peak resistance values are practically identical. The above-mentioned findings indicate therefore that the homogeneity factor is ensured for all the pressuremeter tests performed.

This part presents the results of the multi-cycle tests whose objective was to test the capacity of the developed probe to perform cyclic tests. All the tests were conducted with the Jean Lutz controller. This device allows for a numerical control with enslavement of all the test parameters. The monitoring operation was carried out using a specific software program (PREVO) installed on a laptop and connected to the controller. The software was developed specifically for carrying out cyclic pressuremeter tests (Fig. 20).

Dupla (1995) suggested that the pressure inside the cavity varies according to a sinusoidal signal that is given by the following formula:

$$p_{cav} = p_0 * (1 + Rc * \sin(\omega t)) \;\; ; \;\; \omega = \frac{2\pi}{T} \;\; ; \;\; R_c = \frac{\Delta P_{cyc}}{P_{cav,i}} \quad (3)$$

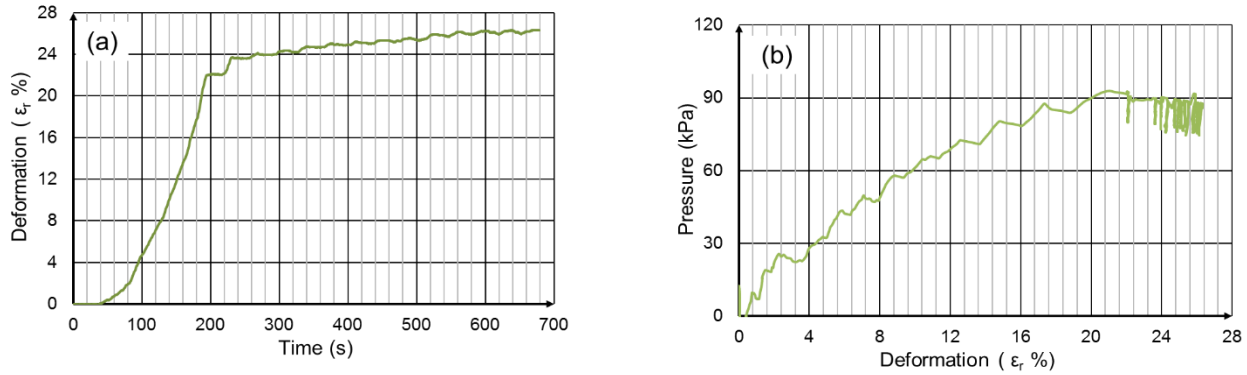

Fig. 24 (a) Curve representing the variation of deformation over time and (b) Pressure-strain curve for the pressure half-amplitude of 8 kPa

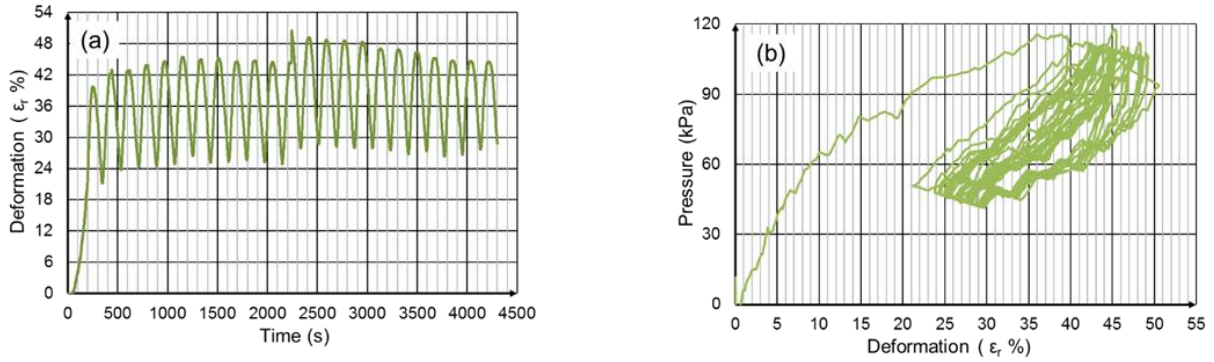

Fig. 25 (a) Curve representing the variation of deformation over time and (b) Pressure-strain curve for the pressure half amplitude of 50 kPa

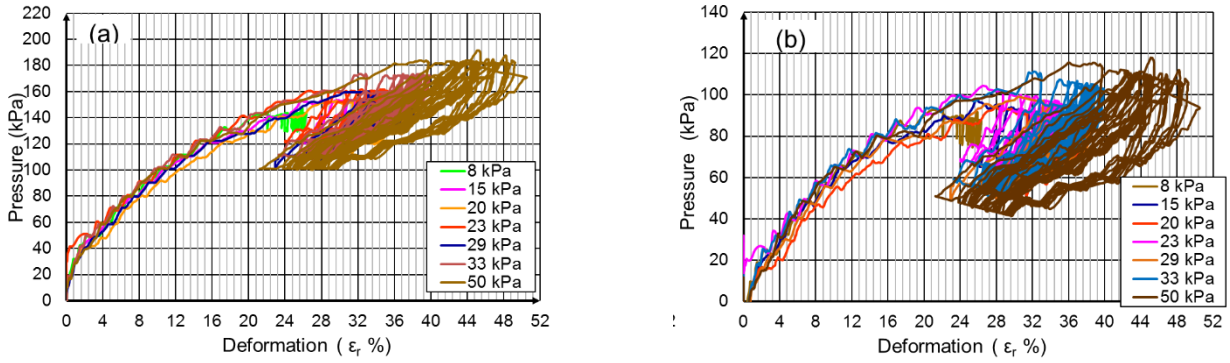

Fig. 26 Results of multi-cycle tests: (a) Raw curves and (b) Corrected curves

where:

P_{cav} is the pressure inside the cavity, P_0 is the horizontal pressure in place, R_c the cyclic stress ratio, ω the pulsation, T the time and ΔP_{cyc} is the half-amplitude pressure.

The magnitude that changes during the tests is the half-amplitude pressure ΔP_{cyc}. It is chosen based on the cyclic stress ratio. The cyclic loading can be either alternated, i.e., the strain deviator oscillates between ± ΔP_{cyc}, or not alternated, if the controlled variable does not change sign during solicitation, as depicted in Fig. 21. The different loading cases tested are shown in Fig. 22.

It is worth noting that Fig. 23 indicates that the servo program functions properly.

One can easily notice that when it comes to small loading cycles, like for example in the case of a half-amplitude where the pressure is equal to 8 kPa, it is difficult to identify the loops in the curve representing the evolution of pressure as a function of radial deformation. This curve has almost no cycles, as it is clearly shown in Fig. 24.

On the other hand, for relatively large cycles, as in the case of a pressure half-amplitude of 50 kPa, the loops are clearly perceptible in the two graphical representations (Fig. 25).

The corrected raw pressure curves as a function of deformation are shown in Fig. 26. The tests previously carried out indicate that the results obtained confirm the good functioning of the developed probe. In addition, this probe makes it possible to perform multi-cycle tests under controlled conditions. However, some problems, such as the noise of recorded signals, still remain. These problems are

usually directly related to the acquisition system. It appears that, for all the tests carried out, a monotonic part exists between zero and the creep pressure that is theoretically not corrected; this is followed by a cyclical phase which is manifested for each cycle around the chosen half-amplitude.

5. Conclusions

This article gives a detailed presentation on the design, manufacture and operation of a new pressuremeter probe which should contribute to better understand soils, particularly with regard to small deformations; it also helps to determine the modulus of elasticity. The probe developed is remarkably different from the conventional Ménard probe, especially in a system for measuring the radial membrane deformation used in a measuring feeler equipped with a Hall Effect sensor instead of deducing the displacements from the volume variations of a fluid. This project suggests interesting perspectives that allow determining highly accurate mechanical characteristics of a soil with better quality, using the developed probe.

The calibration section of the two sensors used in the present study was succinctly presented, after obtaining the mathematical relations that help one to pass from the values in volts to the those in bars or kPa in the case of the pressure sensor, and to the values in mm for the Hall Effect sensor. The multi-cycle tests were carried out under good coherence conditions. This confirms the relevance and performance of the developed probe. This result is fully justified by the cyclic pressuremeter expansion tests with regard to behavior, trend and measurement interval.

Soil behavior response was observed when the cyclic expansions were applied. This new probe makes it possible to determine the parameters describing and quantifying the behavior of soil when subjected to a cyclic loading, with an economic dimensioning of the structures. Future research will certainly show that this equipment may play a major role in the identification and characterization of soils in a seismic context.

References

Akbar, A. (2001), "Development of low cost in-situ testing devices", Ph.D. Thesis, Newcastle-upon Tyne University, Newcastle-upon Tyne, U.K.

Amar, S., Clarke, B.G., Gambin, M.P. and Orr, T.L.L. (1991*), The Application of Pressuremeter Test Results to Foundation Design in Europe*, European Regional Technical Committee No. 4, Pressuremeters, Balkema A.A., 1-24.

Arbaoui, H. (2003), "Mesure de la déformabilité des sols en place avec un pénétromètre [Measurement of the deformability in situ with a penetrometer]", Ph.D. Thesis, Blaise Pascal University, Clermont-Ferrand, Auvergne, France.

Aziz, M. and Akbar, A. (2017), "Interrelationships of flat rigid dilatometer parameters with unconfined compression test results", *Geotech. Test. J.*, **40**(2), 258-268. https://doi.org/10.1520/GTJ20160205.

Baguelin, F. and Jézéquel, J. (1973), "Le pressiomètre autoforeur [The self-boring pressuremeter]", *Bulll. LPC*, **67**, 9-30

Baguelin, F., Jézéquel, J.F. and Shields, D.H. (1978), *The Pressuremeter and Foundation Engineering*, in *Transtech Publications*.

Barry, M.A., Johnson, B.D. and Boudreau, B.P. (2012), "A new instrument for high-resolution in-situ assessment of Young's modulus in shallow cohesive sediments", *Geo-Marine Lett.*, **32**(4), 349-357. https://doi.org/10.1007/s00367-012-0277-z.

Borel, S. and Reiffsteck, Ph. (2006), *Caractérisation de la Déformabilité des Sols au moyen d'Essais en Place [Characterization of Soil Deformability by means of In-situ Tests]*, in *Etudes et Recherches des Laboratoires des Ponts et Chaussées [Studies and Research in the Laboratories of Bridges and Roads, Geotechnical Series]*, Série Géotechnique (In French).

Briaud, J.L. and Shields, D.H. (1979), "A Special pressuremeter and pressuremeter test for pavement evaluation and design", *Geotech. Test. J.*, **2**(3), 143-151. https://doi.org/10.1520/GTJ10446J.

Campanella, R.G. and Robertson, P.K. (1986), "Research and development of the UBC cone pressuremeter", *Proceedings of the 3rd Canadian Conference on Marine Geotechnical Engineering*, Saint Johns, New Foundland, Canada.

Clarke, B.G. (1995), *Pressuremeter in Geotechnical Design*, Blackie Academic and Professional, London, U.K.

Dupla, J.C. (1995), "Application de la sollicitation d'expansion de cavité cylindrique à l'évaluation des caractéristiques de liquéfaction d'un sable[Application of the cylindrical cavity expansion stress to the evaluation of the liquefaction characteristics of a sand]", Ph.D. Dissertation, Ecole des Ponts ParisTech, Paris, France.

Gambin, M.P. (1990), "The history of pressuremeter practice in France", *Proceedings of the 3rd International Symposium on Pressuremeters*. Oxford, U.K., April.

Ghionna, V.N., Jamiolkowski, M., Pedroni, S. and Piccoli, S. (1995), "Cone penetrometer tests in Po River sand", *Proceedings of the 4th International Symposium, the Pressuremeter and its New Avenues*, Sherbrooke, Québec, Canada, May.

Jézéquel, J.F. and Touzé, J. (1970), "Sonde foreuse pressiométrique [Pressuremeter drilling probe]", Patent No. 1.596.747 (In French).

Johnston, G., Doherty, J. and Lehane, B. (2013), "Development of a laboratory-scale pressuremeter", *Int. J. Phys. Modell. Geotech.*, **13**(1), 31-37. https://doi.org/10.1680/ijpmg.12.00011.

Kögler, F. (1933), "Baugrunprufung im Borloch [Ground test in the borehole]", *Der Bauingenieur [The Civil Engineer]*, **19-20** (In German).

Likitlersuang, S., Surarak, C., Wanatowski, D., Oh, E. and Balasubramaniam, A. (2013), "Geotechnical parameters from pressuremeter tests for MRT blue line extension in Bangkok", *Geomech. Eng.*, **5**(2), 99-118. https://doi.org/10.12989/gae.2013.5.2.099.

Masoud, Z. and Khan, A.H. (2019), "An Improved Technique for Prebored Pressuremeter Tests", *KSCE J. Civ. Eng.*, **23**(7), 2839-2846. https://doi.org/10.1007/s12205-019-1448-5.

Ménard, L. (1955), "Pressiomètre[Pressuremeter]", Patent No. 1.117.983 (In French).

Messaoud, F. and Cosentino, P.J. (2016), "Pencel pressuremeter efficiency for data compilation and analysis", *Appl. Mech. Mater.*, Vol. **845**, 100-105. https://doi.org/10.4028/www.scientific.net/AMM.845.100.

Oztoprak, S., Sargin, S., Uyar, H.K. and Bozbey, I. (2018), "Modeling of pressuremeter tests to characterize the sands", *Geomech. Eng.*, **14**(6), 509-517. https://doi.org/10.12989/gae.2018.14.6.509.

Rehman, Z. (2010), "Development of a pressuremeter to operate in alluvial soils of Punjab", Ph.D. Thesis, University of Engineering and Technology, Lahore, Pakistan.

Reid, W.M., John, H.D., Fyffe, S. and Rigden, W.J. (1982), "The Push-In Pressuremeter", *Proceedings of the Symposium on the Pressuremeter and its Marine Applications*, Paris, France, April.

Reiffsteck, Ph. and Borel, S. (2002), "Proposition d'une nouvelle technique d'essai en place: L'appareil triaxial in situ [Proposal for a new test technique in situ: The triaxial device in situ]", *Proceedings of the International Symposium on Identification and Determination of Soil and Rock Parameters for Geotechnical Design*, Paris, France, September (In French).

Reiffsteck, Ph., Reverdy, G., Vinceslas, G. and Sagnard, N. (2005), "Pressiomètre autoforeur de nouvelle génération-PAF2000 [New generation of self-boring pressuremeter-PAF2000]", *Proccedings of the 5th International Symposium on Pressuremeters*, Marne-la-vallée, France, August (In French).

Shaban, A.M. and Cosentino, P.J. (2017), "Development of the miniaturized pressuremeter test to evaluate unbound pavement layers", *J. Test. Eval.*, **45**(2) 521-533. https://doi.org/10.1520/JTE20150322.

Tarawneh, B., Sbitnev, A. and Hakam, Y. (2018), "Estimation of pressuremeter modulus and limit pressure from cone penetration test for desert sands", *Constr. Build. Mater.*, **169**, 299-305. https://doi.org/10.1016/j.conbuildmat.2018.03.015.

Thorel, L., Gaudin, C., Rault, G., Garnier, J. and Favraud, C. (2007), "A cone pressuremeter for soil characterisation in the centrifuge", *Int. J. Phys. Model. Geotech.*, **7**(1), 25-32. https://doi.org/10.1680/ijpmg.2007.070103.

Wang, K., Xu, G., Wang, J. and Wang, C. (2018), "Self-boring in situ shear pressuremeter testing of clay from Dalian Bay, China", *Soils Found.*, **58**(5), 1212-1227. https://doi.org/10.1016/j.sandf.2018.07.007.

Windle, D. and Wroth, C.P. (1977), "In situ measurement of the properties of stiff clays", *Proceedings, of the 9th International Conference on Soil Mechanics and Foundation Engineering*, Tokyo, Japan, July.

Withers, N.J., Schaap, L.H.J. and Dalton, C.P. (1986), "The development of a full displacement pressuremeter", *Proceedings of the International Symposium on Pressuremeter and its Marine Applications*, Texas, U.S.A., May.

Wroth, C.P. and Hughes, J.M.O. (1972), "An instrument for the in-situ measurement of the properties of soft clays", CUED/C, Soils TR13, Report of Departement of Engineering, University of Cambridge, Cambridge, U.K.

Zhou, S. (1997), "Caractérisation des sols de surfaces à l'aide du pénétromètre dynamique léger à énergie variable type PANDA [Characterization of surface soils using the light dynamic variable energy penetrometer type PANDA]", Ph.D. Thesis, Blaise Pascal University, Clermont-Ferrand, France (In French).

Zuidberg, H.M. and Post, M.L. (1995), "The cone pressuremeter: An efficient way of pressuremeter testing", *Proceeidngs of the 4th International Conference on the Pressuremeter and its New Avenues*, Sherbrooke, Québec, Canada, May.